International Journal of Recent Technology and Engineering (IJRTE)
ISSN: 2277-3878 (Online), Volume-9 Issue-1, May 2020

Field Analysis, Distribution and Performance of Sleeve Rotor Induction Motor Taking the Sleeve Rings into Consideration

Omar S. Daif, M. Helmy A. Raouf, A. B. Kotb

Abstract: ***In this paper, the field analysis of the sleeve-rotor induction motor taking the rings effect into consideration is carried out using the Maxwell's field equations. A model in cylindrical coordinates is used to establish the rotor-rings and to solve the air gap magnetic field. The flux density is assumed to be constant through the very small air gap length while the skin effect through the axial rotor length is considered.***

The axial distribution of the air gap flux density, the sleeve current density components and the force density are obtained. The motor performance is carried out taking into account the effects of the sleeve rings performance characteristics.

The effects of design data on the starting torque and the overload capacity of the motor are also considered.

Keywords: induction motor, sleeve-rotor, field analysis, motor performance.

I. INTRODUCTION

Stator of the single-phase induction motor (IM) has been modified to produce two phase motor for different applications [1-3]. Whereas the IM with sleeve-rotor has usual slotted single-phase stator. Its rotor contains a smooth conducting cylinder mounted on an iron core to complete the magnetic circuit. The inner iron in the rotor cylinder is used here as an iron core to decrease the magnetic reluctance. The homogenous sleeve-rotor construction of Fig. 1, allows higher rotational speed compared with the similar conventional slotted rotor.

Some authors have carried out theoretical studies on a sleeve-rotor IM. The effects of the secondary sheet design data on the motor performance characteristics are considered in [4], without taking the effects of the rotor-rings into account. In [5], the rotor ends are taken into consideration for the case of asymmetrical sleeve-ends.

In this paper, the field analysis of the sleeve-rotor IM is carried out using Maxwell's field equations in cylindrical coordinates. The flux density is assumed to remain constant along the very small mechanical air gap length between the stator surface and the sleeve cylinder.

The current density through the conducting sleeve is allowed to have both axial and tangential components.

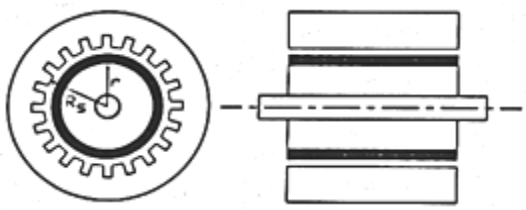

Fig. 1. Sleeve-rotor induction motor

The axial distribution of the air gap flux density as well as the sleeve-rotor current density components are obtained taking sleeve-rings into consideration [6]. These components are calculated and plotted, at different rotor speeds. The main performance characteristics of the motor are determined and the effects of the sleeve-rings are discussed.

II. MODEL OF SLEEVE-ROTOR IM WITH SLEEVE-RINGS

A simple model in cylindrical coordinates is used to establish the rotor-rings and to solve the air gap magnetic field. The magnetic flux is assumed to remain radially constant through the very small air gap length. The two components of the rotor current density are considered through the active sleeve length, taking into account the effects of the sleeve-rotor rings. The model shown in Fig. 2 will be used with the assumptions of infinitely permeability and zero conductivity for the iron parts. The stator windings are replaced in this model by an equivalent current sheet of infinitesimal thickness, carrying the stator electric loading $\boldsymbol{A_s}$. The two rotor-rings have the same sleeve conductivity with larger width as shown in Fig. 2.

According to the mentioned assumptions; the air gap flux density $\boldsymbol{B_r}$ will has only a radial component:

$$\vec{\boldsymbol{B}} = \boldsymbol{B_r} \cdot \vec{\boldsymbol{a}}_r \qquad (1)$$

The sleeve-rotor has both axial and tangential current density components $\boldsymbol{J_z}$ and $\boldsymbol{J_\varphi}$ respectively.

Manuscript received on April 02, 2020.
Revised Manuscript received on April 20, 2020.
Manuscript published on May 30, 2020.

* Correspondence Author
Omar S. Daif*, M. Sc. in Electrical Engineering, Al-Azhar University, Cairo, Egypt. Email: omareng2006@gmail.com
M. Helmy A. Raouf, Department of Electrical Quantities Metrology, National Institute of Standards (NIS), Giza, Egypt. Email: mohammed_makka@yahoo.com
A. B. Kotb, Department of Electrical Engineering, Al-Azhar University, Cairo, Egypt. Email: moabdelsamie45@yahoo.com

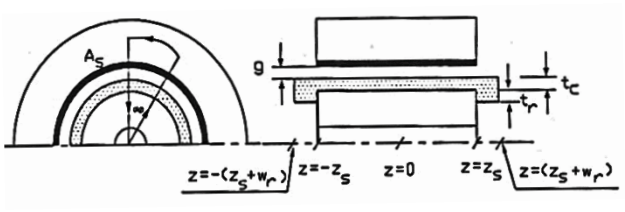

Fig. 2.Model for sleeve-rotor IM with sleeve-rings.

III. FIELD ANALYSIS

By applying the integral form of the Maxwell's first equation to a loop of infinitesimal dimensions in r - φ plane in the model illustrated in Fig. 2, then:

$$\frac{\partial B_r}{\partial \varphi} = \frac{\mu_o}{g_s}(R_s A_s + r t_c J_z) \quad (2)$$

Where R_s is the inner stator radius, r is the iron rotor radius, t_c is the sleeve thickness and $g_s = g + t_c$.

The stator electric loading wave A_s can be expressed in a complex form as:

$$A_s(\varphi, t) = R_e\left(\underline{\hat{A}}_s\, e^{j(\omega t - p\varphi)}\right) \quad (3)$$

With $p\varphi$ in electrical degree, where p is the number of stator pole pairs and an angle φ is in mechanical degree. The stator electric loading wave, A_s has both time t and an angle φ functions. The restriction to steady state operation allows the representation of the field quantities to be:

$$B_r(\varphi, t, z) = Re\left(\underline{\hat{B}}_r(z)\, e^{j(\omega t - p\varphi)}\right) \quad (4)$$

$$J_z(\varphi, t, z) = Re\left(\underline{\hat{J}}_z(z)\, e^{j(\omega t - p\varphi)}\right) \quad (5)$$

By substituting Eqs. 3, 4, 5 into Eq. 2, the air gap flux density is then:

$$B_r(z) = j\frac{\mu_o R_s}{p g_s} A_s + j\frac{\mu_o t_s r}{p g_s} J_z \quad (6)$$

The current density in an isotropic medium moving with a velocity $\vec{v}$, is:

$$\vec{J} = \sigma_c(\vec{E} + \vec{v} \times \vec{B}) \quad (7)$$

Where $\vec{E}$ is the electric field intensity induced by transformer action, $\vec{v}$ is the liner rotor speed and σ_c is the sleeve material conductivity.

The second Maxwell's equation can be applied to the closed loop of Fig. 2, in the φ, Z-plane to obtain:

$$\frac{\partial J_\varphi}{\partial z} + j\frac{p}{r} J_z = j\omega\sigma_c S B_r \quad (8)$$

Where S is the slip = (1 – (n/n_s)), with n is the rotor speed and n_s is the synchronous speed.

The relation between φ and Z-components of the rotor current density can be obtained by the continuity condition:

$$div\, J = 0.0, and\ then\ J_\varphi = -j\frac{r}{p}\cdot\frac{\partial J_z}{\partial z} \quad (9)$$

From the previous relations, the axial component of the rotor current density is governed by the following second order differential equation:

$$\frac{\partial^2 J_z}{\partial z^2} - \left(\frac{p^2}{r^2} - j\frac{\omega\sigma_c s\mu_o t_c}{g_s}\right) J_z = -j\left(\frac{\omega\sigma_c s\mu_o R_s}{g_s r}\right) A_s \quad (10)$$

The differential equation (10), describes the axial component of the rotor current density.

A convenient general solution for the complex amplitude of J_z is:

$$J_z = D_1 e^{kz} + D_2 e^{-kz} + \left(j\frac{\omega\sigma_c s\mu_o R_s}{g_s r k^2}\right) \quad (11)$$

Where the complex quantity,

$$k^2 = \frac{p^2}{r^2} - j\left(\frac{\omega\sigma_c s\mu_o t_c}{g_s}\right) \quad (12)$$

The unknown complex constants D_1 and D_2 can be determined by applying the boundary conditions: $J_z = 0$ at the edge of each rotor-ring, i.e. (z = ± (z_s + w_r)). For the symmetrical rotor rings, the two unknown complex constants D_1 and D_2 will be only one constant, D.

The current density transition from the rotor active length to the sleeve-rotor rings is illustrated in Fig. 3.

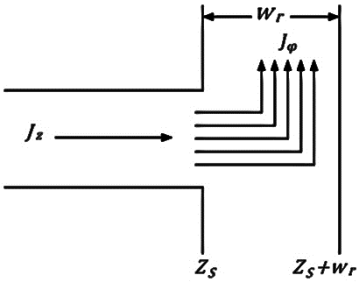

Fig. 3.Transition of the rotor currents to the sleeve rings.

The φ – component of the current density in the sleeve-rings is assumed constant all over each rotor ring width. The axial current density component J_z turns to be tangential through the rotor rings. The continuity equation at one rotor end is then:

$$J_z(z_s) = \frac{W_r^{\backslash}}{r}\frac{\partial J_\varphi}{\partial \varphi}\bigg|_{z=z_s} \quad (13)$$

Where W_r is the ring width and t_r is the ring thickness, then the effective ring width is $W_r^{\backslash} = W_r\frac{t_r}{t_c}$.

Applying the diversion theorem to give:

$$\frac{1}{r}\frac{\partial J_\varphi}{\partial \varphi} = -\frac{\partial J_z}{\partial z} \quad (14)$$

Hence the unknown constant D can be expressed as:

$$D = \frac{\left(j\frac{\omega\sigma_c s\mu_o R_s}{g_s r k^2}\right) A_s}{e^{kz_s} + e^{-kz_s} \cdot kW_r^{\backslash} \cdot (e^{kz_s} - e^{-kz_s})} \quad (15)$$

Substituting Eq. 15 in Eq. 11 yields,

$$J_z(z) = \left(1 - \left(\frac{e^{kz} + e^{-kz}}{(e^{kz_s} + e^{-kz_s}) + kW_r^{\backslash} \cdot (e^{kz_s} - e^{-kz_s})}\right)\right) \cdot \left(j\frac{\omega\sigma_c s\mu_o R_s}{g_s r k^2}\right) A_s \quad (16)$$

The tangential component of the sleeve current density is then,

$$J_\varphi(z) = -\frac{\omega\sigma_c s\mu_o R_s}{pkg_s} A_s \cdot \left(\frac{e^{kz} - e^{-kz}}{(e^{kz_s} + e^{-kz_s}) + kW_r^{\backslash} \cdot (e^{kz_s} - e^{-kz_s})}\right) \quad (17)$$

Also, the air gap flux density is:

$$B_r(z) = j\frac{\mu_o R_s}{p g_s} A_s \left(1 + \left(\left(j\frac{t_c\omega\sigma_c s\mu_o}{k^2 g_s}\right) \cdot \left(1 - \left(\frac{e^{kz} + e^{-kz}}{(e^{kz_s} + e^{-kz_s}) + kW_r^{\backslash} \cdot (e^{kz_s} - e^{-kz_s})}\right)\right)\right)\right) \quad (18)$$

The air gap flux density and the sleeve-rotor current density are important quantities for all of the design procedures and their product is directly related to the developed power density.

Once, the axial rotor current density and the air gap flux density are known, then the tangential force per unit sleeve volume can be expressed as:

$$f_{v\varphi} = -\frac{1}{2} R_e \left(\hat{J}_z^* \cdot \hat{B}_r \right) \qquad (19)$$

IV. CALCULATIONS AND RESULTS:

The selected normal design data for the following computed curves are:

f = 50 Hz, p = 2.0, $2Zs$ = 8 cm, r = 3.75 cm, g = 0.2 mm, t_c = 0.5 mm, $\sigma_c = 5 \times 10^7 \frac{1}{\Omega.m}$, W_r = 10 mm, t_r=2.5 mm.

The axial distribution of the two sleeve current density components, the air gap flux density and the tangential force density are calculated and plotted in Figs. 4-7, with a rotor without sleeve-rings; i.e. W_r and t_r are equal to zero.

The distributions are normalized by the following base quantities; for the current density components (A_s/t_c), for the air gap flux density $(\mu_o R_s A_s/pg_s)$ and for the force density $(½\ \mu_o R_s A_s^2/pg_s t_c)$ which are suitable bases for the normalization.

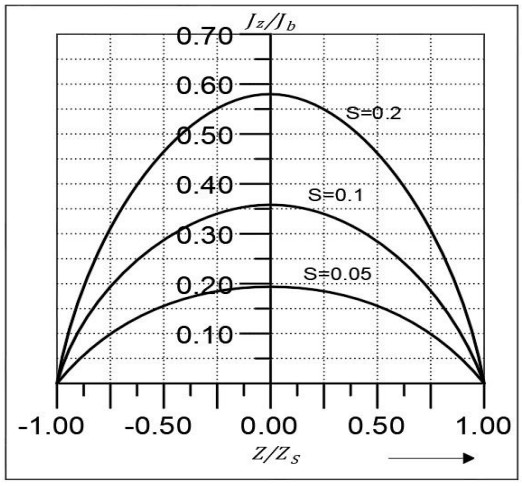

Fig. 4.Axial current density distribution without rings.

Three families of curves are given for three different speeds to illustrate the effects of the sleeve-rotor armature reaction on the field distribution. The axial distributions without sleeve-rings are shown in those figures through the motor speed range.

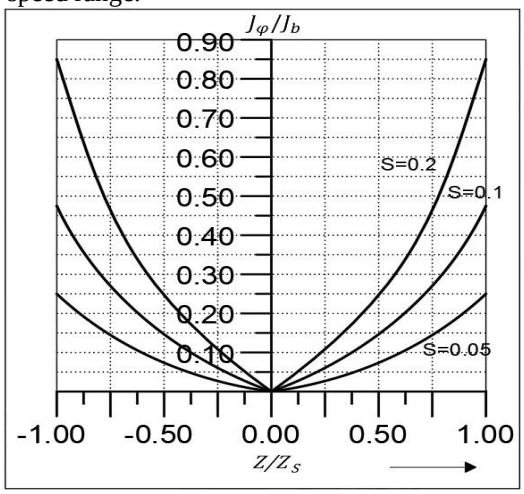

Fig. 5.φ-current density distribution without rings.

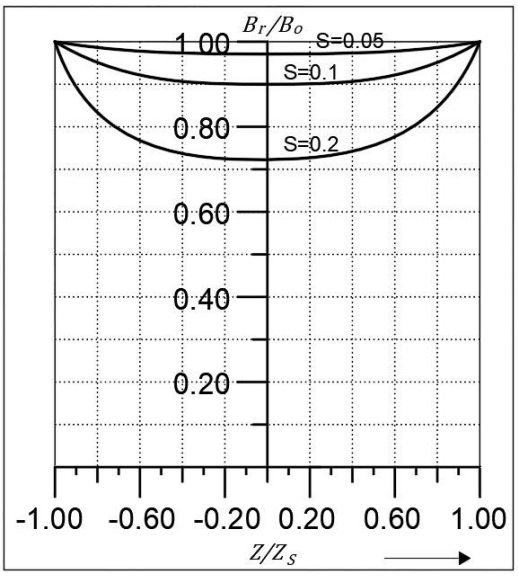

Fig. 6. Radial flux density distribution without rings.

At the middle of the sleeve-rotor, the axial component of the sleeve current density attains its maximum value, while the tangential component reduces to zero. The maximum value of the axial current density component increases with the increasing the slip.

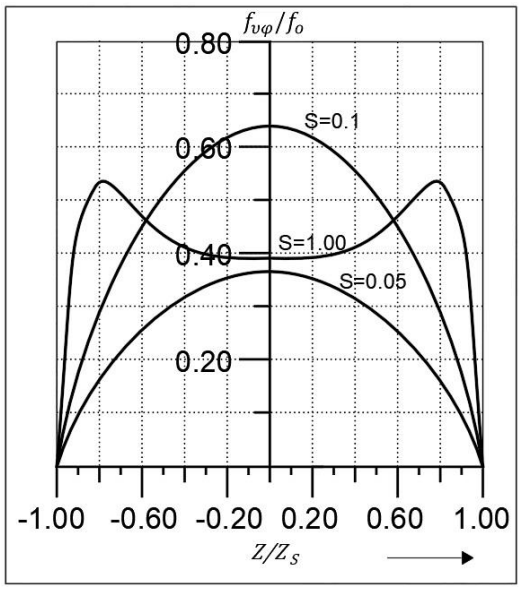

Fig. 7.Force density distribution without sleeve rings.

The difference between the no load and full-load flux density is the immediate measure of the intensity of the rotor armature reaction.

At full-load speed, the maximum force density occurs in the middle of the rotor sleeve with its contribution to the developed torque will be large. At the motor starting, the maximum force density appears near to the rotor edges and its effect on the starting toque will be weaker.

Figures 8-11 show the computed axial distribution of sleeve current density components, air gap flux density and tangential force density but with sleeve-rings.

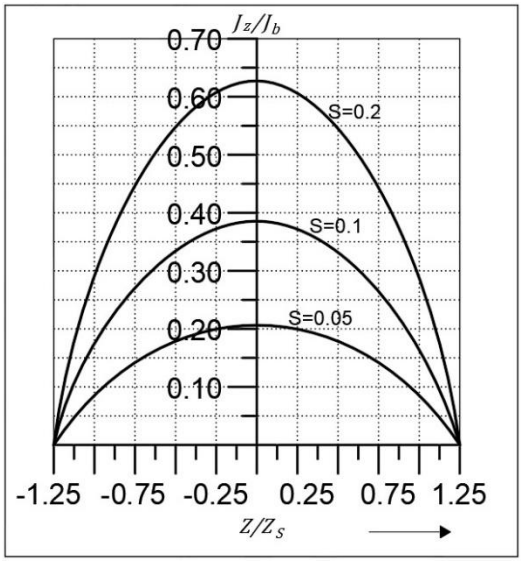

Fig. 8.Axial current density distribution with sleeve rings.

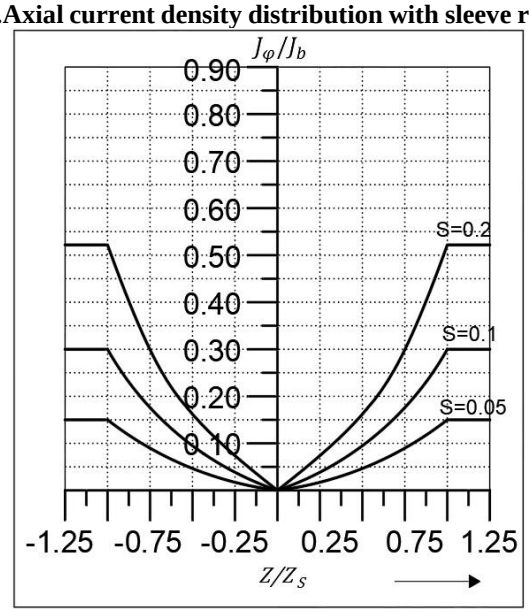

Fig. 9.φ-current density distribution with sleeve rings.

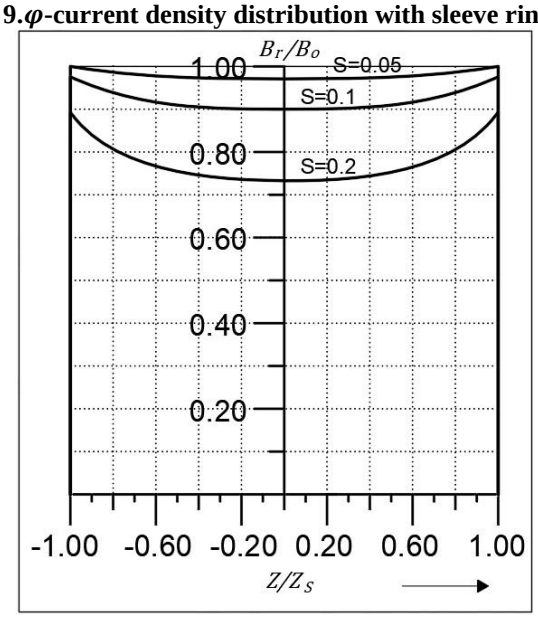

Fig. 10. Radial flux density distribution with sleeve rings.

As a result of sleeve rings, the field components have more flatted distributions than that of the previous case without sleeve rings. This is due to the current loops, which close their paths within the sleeve-rings instead of closing the eddy current loops through the main sleeve region. It is clear that the tangential component of the sleeve-current density is constant all over the ring width.

It is obvious that, the contribution of the force density to the developed torque, will has an expected higher value. This will lead to a better characteristic performance for the motor with sleeve rings than that without sleeve-rings.

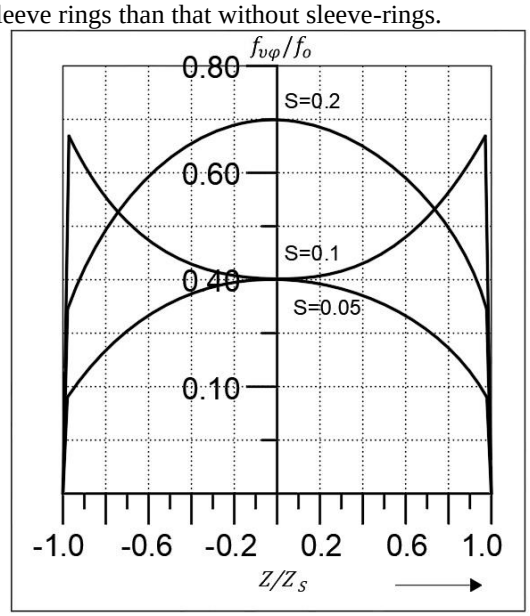

Fig. 11. Force density distribution with sleeve rings.

The torque density acting on the rotor sleeve can be obtained directly from the force density multiplied by the sleeve radius r as:

$$\boldsymbol{T_{qv} = f_{v\varphi} \cdot r} \qquad (\mathbf{20})$$

The total torque acting on the rotor can be obtained by integrating the torque density over the sleeve volume. The developed torque is then:

$$\boldsymbol{T_q = 2\pi r^2 \cdot t_c \cdot \int_{-z_s}^{z_s} f_{v\varphi}\, d_z} \qquad (\mathbf{21})$$

Figure 12, shows the computed torque-speed characteristics for two rotors, one without sleeve-rings and the other with sleeve-rings. The base value of the torque is taken as $(4\pi \boldsymbol{r^2} t_c z_s)$ times the force density base.

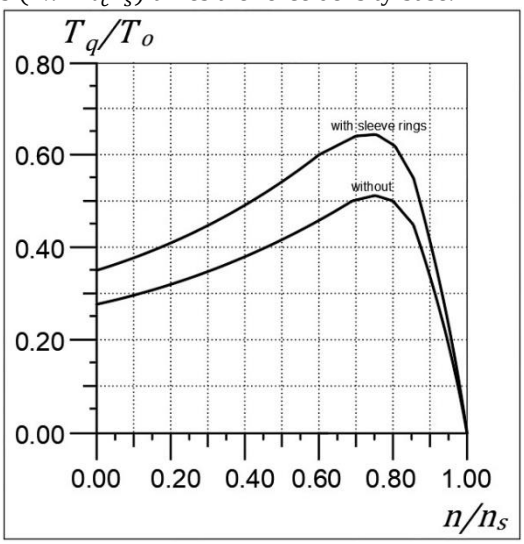

Fig. 12. Torque-speed characteristics with and without sleeve rings.

The motor with sleeve-rings has an improved performance characteristic with higher developed torque through the operating range. As expected, this is due to the current loops which close their paths within the sleeve-ring region. It is evident that the current displacement phenomenon with respect to the axial direction takes place in the rotor conducting sheet.

Some effects of the sleeve-rotor design data on the motor performance are demonstrated by comparing the characteristics of four sleeves for the considered motor. The different curves of Fig. 13, are obtained from the combinations of sleeves with normal design data as base and decreasing the sleeve thickness, the sleeve conductivity and decreasing the air gap length.

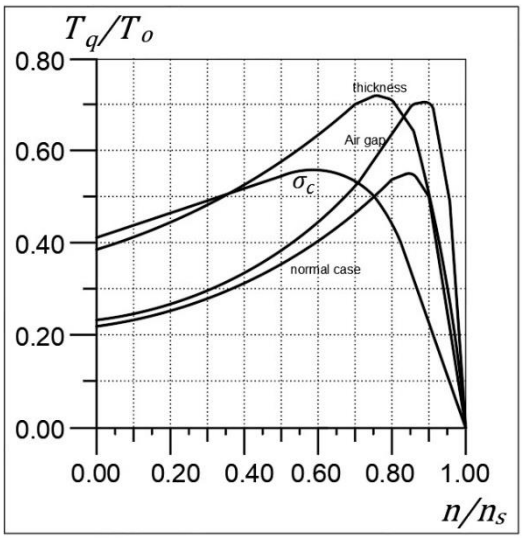

Fig. 13. Torque speed characteristics for different sleeve design data, $t_c = 0.5 \cdot t_{cn}$, $g = 0.5 \cdot g_n$, $\sigma_c = 0.4 \cdot \sigma_{cn}$.

As shown in Fig.13, the thickness of the sleeve sheet affects the developed torque at normal operation with better starting conditions. The sleeve thickness is limited by predetermined maximum current density for avoiding the material heating.

The aluminum sleeve with normal sleeve dimensions, gives higher starting torque than that of the copper sleeve. Decreasing the air-gap length provides a higher maximum torque. The mechanical consideration is only the constraint for using the shortest air gap length, which is the same limit for any cylindrical rotor machine.

V. CONCLUSIONS:

The model and analysis of the sleeve-rotor induction motor with rotor rings, using cylindrical coordinates restore the geometry of the machine. It is evident that the current displacement phenomenon with respect to the axial direction takes place in the sleeve conducting sheet.

The sleeve rings improve the motor characteristics and increase the developed torque through the operating range.

The predicated results show that it is better to design the rotor sleeve with thin sheet and shorter air gap, which allows considerable improvements in the motor performance with saving in the active materials.

REFERENCES

1. Ayman Ali, Salama Abo Zayd, Abdel Samie Kotb. “Two- Phase Induction Motor Fed from Solar Power via Programmed Wave Inverter” IJOSER. Vol. 8, Issue 5, 2017.
2. Sara Ali, M. Adel, A. B. Kotb. “Two Phase Motor Fed From Single Phase Supply, Using Control Circuit” JOAUES. Vol. 14, No. 52, 2019.
3. H. I. Shousha, A. B. Kotb, M. Elwany. “Two Phase Motor Under Control” IJRTE. Vol. 8, Issue 3, 2019.
4. A. B. Kotb, “The Effects of Secondary Sheet Design on the Performance of Sleeve-Rotor Induction Motor” AEC. 1. Vol. 9, PP. 47-55, 1989.
5. A. B. Kotb, “Sleeve-Rotor Induction Motor with Rotor Ends” Record of the fifth International Middle East Power Conference MEPCON 97, PP. 170-175, Jan 4-6, 1997.
6. M. A. Elwany, A.G. Abou-Arafa and M. Helmy A. Raouf, “Sleeve-Rotor Induction Motor with Rotor-Rings”, Al-Azhar Engineering 7th International Conference, AEIC 2003, Code E07102, Cairo, Egypt, 7-10 April, 2003.

AUTHORS PROFILE

Omar Sobhy Daif, received the B. Sc. and the M. Sc. in Electrical Engineering from the Faculty of Engineering, Al-Azhar University, Cairo, Egypt in May 2009 and May 2018, respectively. In 2012 he became senior engineer of Testing Department at Cairo Oil Refining Company (CORC), Egypt. Since 2013, he has been a Head of Department of the Electrical service. From 4/2014 until now he works as summer training lecturer and instructor for Electrical courses at CORC training Department. He works in design and build 2 main substations (11/0.4 KV – 4MVA) and upgrade one main substation (66/11 KV – 130MVA). His research interests are mainly in the electrical machines and Energy Efficiency.

Mohammed Helmy Abd El-Raouf, received the B. Sc., the M. Sc., and the Ph. D. in Electrical Engineering from the Faculty of Engineering, Al-Azhar University, Cairo, Egypt in May 2001, January 2005 and 2007, respectively. In 2018 he became full Professor. He joined the National Institute of Standards (NIS), Egypt, in 2003. From 4/2010 to 4/2011 he was Post – Doctor at Korea Research Institute of Standards and Science (KRISS), Deajeon, South Korea. Since 2013, he has been a Head of Department of the Electrical Quantities Metrology at NIS. Since 2016, he is the vice chair, of the Technical Committee for Electricity and Magnetism (TC-EM) of AFRIMETS, the intra-Africa metrology system, and the Egyptian delegate to the Consultative Committee for Electricity and Magnetism (CCEM) of the International Committee for Weights and Measures (CIPM). His research interests are mainly in the electrical machines and metrology of the electrical quantities such as capacitance, inductance, resistance, impedance and AC-DC measurements. He published about 40 papers in refereed scientific journals and has 6 patents. He teaches some courses in electrical engineering.

A. B. Kotb, Prof. Dr. Abd El-Sameea Basuny Kotb, Professor of Electrical Machines, Faculty of Engineering Al-Azhar University. His research interests are mainly in the electrical machines and their applications.